

Radionuclides Differentiation during the Secondary Processes of Pb-Zn Mineralization, Gabal El Rousas, Eastern Desert, Egypt

Sh.M.Talaat¹ and A.I.M.Ismail²

¹ Faculty of Women, for Art, Science and Education, Ain Shams University, Cairo, Egypt.

² Geological Science Department, National Research Center, Dokki, Cairo, Egypt.

Shadia_talaat@yahoo.com

Abstract: The primary mineralization of Pb-Zn in Gabal El Rousas on the Egyptian Red Sea hills was subjected to secondary processes led to the redistribution of those mineralization and became much abundant than the hypogene minerals. This study is restricted on the differentiation in the associated radionuclides during these secondary processes. Seven samples from the mineralized ore and six samples from the hosting Miocene sedimentary rocks were collected and studied radiometrically using the Hyper Pure Germanium (HPGe) detector. The results showed that the ²³⁸U and ²²⁶Ra are concentrated in the hosting rocks, while ⁴⁰K on the other hand is concentrated in the mineralized zones. ²³²Th did not change much due to its immobility, while in the mineralized group, ²¹⁴Pb and ²¹⁴Bi are nearly half the activity concentration of their parent ²²⁶Ra which is due to the escape of some ²²²Rn during the secondary processes that affected the primary mineralization. With respect to the environmental impact, the absorbed dose rate, annual effective dose rate, radium equivalent, radioactivity level index and external radiation hazard index for the mineralized samples are three times lower than the hosting sedimentary rocks.

[Sh.M.Talaat and A.I.M.Ismail **Radionuclides Differentiation during the Secondary Processes of Pb-Zn Mineralization, Gabal El Rousas, Eastern Desert, Egypt** *Life Sci J* 2012;9(4):2857-2864] (ISSN:1097-8135). <http://www.lifesciencesite.com>. 419

Keywords: Gabal El Rousas / Gamma ray spectroscopy/ Natural radioactivity / Radiation hazard indices

1. Introduction

As a result of the activity concentration of primordial radionuclides ²³⁸U, ²²⁶Ra, ²³²Th series, and ⁴⁰K that exist in air, water, human's body, food, building supplies and earth's coating, many creatures have exposed to such natural radiation⁽¹⁾. There is a wide broaden existence of natural radioactivity in the earth surroundings and in different geological structures, rocks, water, air and soils⁽²⁾. Such concentrations are not identical all over the world; they broadly fluctuate with diverse locations. The present study aims to discuss the distribution and differentiation of the main radionuclides; ²³⁸U, ²²⁶Ra, ²¹⁴Pb, ²¹⁴Bi, ²³²Th and ⁴⁰K in the mineralized and hosting rocks at Gabal El Rousas area, Eastern Desert, Egypt. The environmental background level of natural radiation, dose rate, annual effective dose, radium equivalent activity, radioactivity level index and external hazard were investigated. The X-Ray Diffraction (XRD) tests for two representative samples are carried out.

Regional Setting

Gabal El Rousas (lead Mountain) area is located at longitude 34° 46' E and latitude 25° 11' N. It is located about 120 km south of Al Quseir (Fig.1a), 16 km north of Marsa Alem and about 7 km west Red Sea coast. Gabal El Rousas proper is an isolated low hillock (Fig.1b) dissected by shallow blind gullies. The maximum elevation is 111 m, and

its relief is about 17 m. It is flat topped and is mostly capped by terrace gravels and sands that cover the Miocene limestone bed rocks⁽³⁾.

The bed rocks of Gabal El Rousas are the limestone and vaporates which covered by gravel terraces and overlies the basement rocks. Gabal El Rousas is characterized by major and minor faults with small displacements (Fig. 1b). The Pb-Zn mineralizations are intense in the major fault zones with epigenetic minerals and their oxidation products⁽⁴⁾. The secondary minerals are abundant which indicate intense alteration processes.

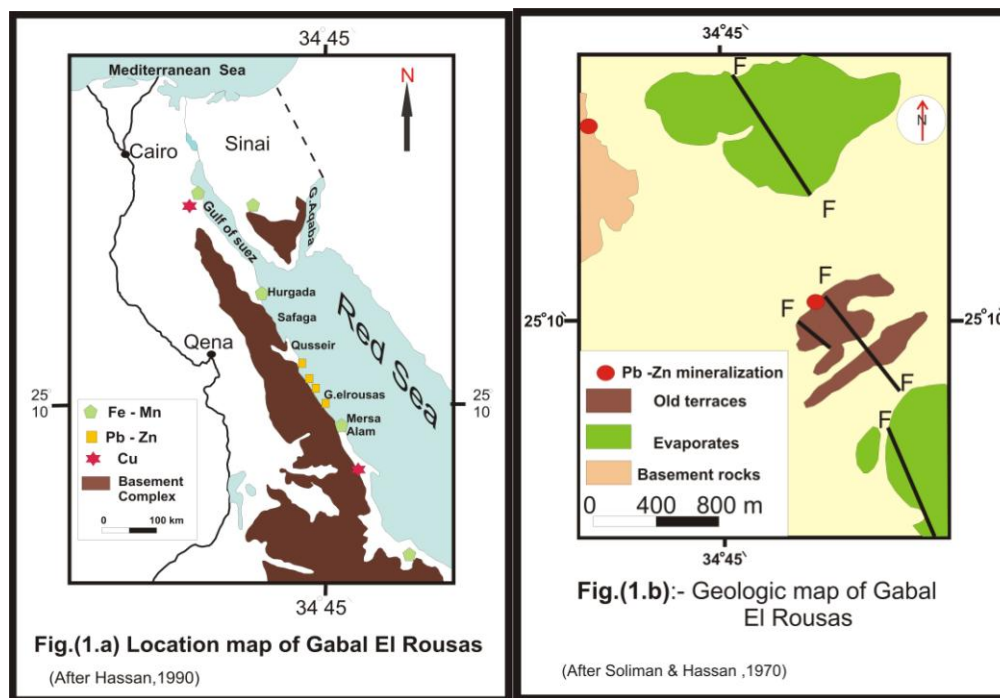
Analytical Technique

Samples collection and preparation

Thirteen representative samples from two sites (1 and 2) were collected from the mineralized bed rocks. The samples from site 1 (seven samples) represent the mineralized group. The samples from site 2 (six samples) are the non-mineralized group. All these samples were dried, trodden, homogenized, weighted and transferred to polyethylene marinelli beakers having volumes of 100 ml and 250 ml. In order to allow for ²²⁶Ra and its short-lived progenies to reach radioactive equilibrium and to make sure that radon gas is confined within the volume and also the daughters remain in the samples, these samples were sealed for a approximate period of four weeks before counting using gamma ray spectroscopy⁽⁵⁾. Each sample was measured during an accumulating time

between 20 hours and 24 hours. After that an empty cylindrical plastic container (polyethylene marinelli beaker) was placed in the detection system, for a

counting period of 48 hours, in order to collect the background count rates.



Figures: (1a and 1b): Location and geological maps of the studied area

2- Experimental techniques.

Two techniques are used in this study; the first is the Hyper Pure Germanium (HPGe) detector for gamma (γ) analysis of all samples. The second is the X-Ray Diffraction (XRD) analysis for two samples; one from each group to identify the mineral constituents. Mineralogical analysis involved (XRD) using a diffractometer BRUKUR D₈ ADVANCE using CuK α radiation with secondary monochromator ($\gamma = 1.5405 \text{ \AA}$). The X-ray tube was operated at 40 Kv and 40 mA. The diffraction angle; two theta (2θ) was scanned at a rate of 2° min^{-1} .

The high purity germanium (HPGe) detector was used for the measurements of gamma ray spectroscopy. The HPGe detector, model (GEM-50210-P), a P-type crystal, from EG & G ORTEC was used for gamma-ray measurements. This detector has a resolution (FWHM) of 1.9 keV for the 1332 keV gamma-ray line of ^{60}Co and a relative efficiency of about 50%. The efficiency calibration for the HPGe detector was carried out by using a ^{152}Eu point source to obtain a broad energy range (from 121.78 to 1408 keV). The relative efficiency curve was normalized for the 100 ml capacity marinelli beakers and for a 250 ml capacity polyethylene container by three different concentrations of chemically pure potassium chloride solution in distilled water. The

absolute efficiency curves were obtained for each size. Activity concentrations were averaged from photopeaks at several energies. The $^{234\text{m}}\text{Pa}$ activities determined from the 1001 Kev photo peak was assumed to represent actual ^{238}U ⁽⁶⁾. The activity concentration for ^{226}Ra was derived from the gamma-ray transition of ^{226}Ra (186.1 keV), for ^{214}Pb (351.9, 295.1 keV) and (609.3, 1120.3, 1764.5 keV) for ^{214}Bi . While the activity concentration of ^{232}Th series was derived from the gamma-ray transition of ^{228}Ac (338.4, 911 keV) and ^{208}Tl (583.1, 2614.4 keV). ^{40}K was determined from the 1460 keV photo peak ⁽⁷⁾. Also XRD analysis measurements were performed which was made at the National Research Center, Dokki, Cairo, Egypt.

Radioactivity Counting

The computation of the activity concentration C (Bqkg^{-1}) for each of the radionuclides in the understudied samples was calculated by using the net area count after the background corrections for each photo peak- knowing that the counting time for each sample was approximately 24 hours using the following expression ⁽⁸⁾:

$$C(\text{Bqkg}^{-1}) = \frac{C_n}{\varepsilon P_\gamma M_s} \quad (1)$$

where C_n is the count rate under each photo peak due to each radionuclide, ϵ represents the detector efficiency for the specific γ -ray, while P_γ is the absolute transition probability of the specific γ -ray and lastly M_s is the mass of the sample (kg).

The following relation was used to obtain the lowest limits of detection (LLD) ⁽⁹⁾:

$$LLD = \frac{4.66 S_b}{\epsilon \times I_\gamma} \quad (2)$$

where S_b is the estimated standard error of the net background count rate in the spectrum of the radionuclide, ϵ represents the counting efficiency and I_γ is the abundance of gamma emissions per radioactive decay. The LLD value for ^{238}U was obtained to be 1.307 Bqkg⁻¹ while that of ^{232}Th and ^{40}K were 1.344 and 9.347 Bqkg⁻¹ respectively.

Hazard Indices

The activity concentrations of ^{238}U , ^{232}Th and ^{40}K measured in each of the studied samples indicate the quantity of radioactivity present but do not provide a measure of radiation risk in the form of an absorbed dose rate. The absorbed dose rate, D (nGyh⁻¹) in air at 1 m above ground level due to the presence of ^{238}U , ^{232}Th and ^{40}K in the studied samples was calculated using the following equation ⁽¹⁾:

$$D(\text{nGyh}^{-1}) = 0.462 A_{Ra} + 0.604 A_{Th} + 0.0417 A_K \quad (3)$$

where A_{Ra} , A_{Th} and A_K are the average specific activities of ^{226}Ra , ^{232}Th and ^{40}K in Bqkg⁻¹ respectively.

The annual effective dose (E_{eff}): The annual effective dose equivalent was calculated from the absorbed dose by applying the dose conversion factor of 0.7 SvGy⁻¹ and the outdoor occupancy factor of 0.2⁽¹⁾. The effective dose rate in units of mSv per year was calculated using the following formula:

$$\text{Outdoor annual effective dose} = D \times 8760 h \times 0.2 \times 0.7 (\text{SvGy}^{-1}) \times 10^{-6} \text{ mSvyr}^{-1} \quad (4)$$

Radium Equivalent Activity (Ra_{eq}): The term radium equivalent represents the weighted sum of the individual activities of ^{226}Ra , ^{232}Th and ^{40}K based on the assumption that 10 Bqkg⁻¹ of ^{226}Ra , 7 Bqkg⁻¹ of ^{232}Th or 130 Bqkg⁻¹ of ^{40}K produce the same gamma-ray dose rates which is calculated using the following relation ⁽¹⁰⁾.

$$Ra_{eq} = A_{Ra} + 1.43 A_{Th} + 0.07 A_K \leq 370 \quad (5)$$

where A_{Ra} , A_{Th} and A_K are the specific activities of ^{226}Ra , ^{232}Th and ^{40}K in Bqkg⁻¹, respectively.

Radioactivity level index (I_γ): The radioactivity level index is used to estimate the level of radiation risk especially gamma ray, associated with natural radionuclide in specific materials. Its definition as follows ⁽¹¹⁾:

$$I_\gamma = A_{Ra}/150 + A_{Th}/100 + A_K/1500 \leq 1 \quad (6)$$

where A_{Ra} , A_{Th} and A_K are the specific activities of ^{226}Ra , ^{232}Th and ^{40}K in Bqkg⁻¹, respectively.

The external hazard index (H_{ex}): The external hazard index (H_{ex}) is the quantity of radium equivalent activity after modification, which is defined as follows ⁽¹⁰⁾:

$$H_{ex} = A_{Ra}/370 + A_{Th}/259 + A_K/4810 \quad (7)$$

Where A_{Ra} , A_{Th} and A_K are the specific activities of ^{226}Ra , ^{232}Th and ^{40}K in Bqkg⁻¹, respectively. The value of H_{ex} must be lower than unity in order to keep the radiation hazard insignificant.

3-Results and Discussions

Radionuclides Distribution

^{238}U activity was determined indirectly from the gamma rays emitted by its daughter products ⁽¹²⁾. The activity of ^{238}U cannot be directly determined, since the isotope emits only a weak (0.064%) gamma-ray at 49.55 keV. However, any of the gamma-emitting daughter nuclides in equilibrium with ^{238}U such as ^{234}Th or ^{234m}Pa could be used for this purpose ^(13, 14). The daughter radionuclides (^{234}Th and ^{234m}Pa) were selected as an indicator of ^{238}U activity. Progeny of ^{238}U are relatively short-lived, and thus it is reasonable to calculate gamma radiations of this sequence as ^{238}U . Therefore, secular equilibrium was assumed between ^{238}U and ^{234}Th and ^{234m}Pa , and thus ^{234m}Pa activities determined from the 1001 keV photo peak, was assumed to represent actual ^{238}U activities⁽⁶⁾. The specific activity of ^{40}K was measured directly by its own gamma-ray at 1460.8 keV, while activities of ^{232}Th series was calculated based on the mean value of its respective decay products which are in secular equilibrium. The specific activity of ^{226}Ra was measured using the 186.1 keV from its own gamma-ray (after the subtraction of the 185.7 keV of ^{235}U).

The results represented by the specific activity (Bqkg⁻¹) of different radionuclides in the studied samples for both sites are presented in table1. Table1 (site1) shows the activity concentrations for ^{226}Ra ranging from 28.80 ± 3.58 Bqkg⁻¹ to 43.10 ± 8.18 Bqkg⁻¹ with an average of 34.49 ± 5.47 Bqkg⁻¹, while it is from 5.84 ± 0.66 Bqkg⁻¹ to 8.73 ± 1.26 Bqkg⁻¹ with an average of 7.31 ± 0.88 Bqkg⁻¹ for ^{232}Th and from 321.59 ± 3.50 Bqkg⁻¹ to 399.96 ± 5.38 Bqkg⁻¹ with an average of 347.73 ± 4.15 Bqkg⁻¹ for ^{40}K . These three averages are in agreement with the world wide values documented at 35, 30, and 400 Bqkg⁻¹ for ^{226}Ra , ^{232}Th , and ^{40}K respectively ⁽¹⁾. It can be also noticed that in Table 1 (site1), the activity concentrations of ^{226}Ra are nearly two times the values for its daughters; ^{214}Bi and ^{214}Pb .

Table 1 (site 2) shows the activity concentration of ^{238}U ranging from $160.94 \pm 24.33 \text{ Bqkg}^{-1}$ to $237.75 \pm 24.23 \text{ Bqkg}^{-1}$ with an average of $201.84 \pm 25.77 \text{ Bqkg}^{-1}$, this average is in disagreement with the worldwide value which is documented at 35 Bqkg^{-1} ⁽¹⁾, while it is ranging from $172.49 \pm 9.87 \text{ Bqkg}^{-1}$ to $209.78 \pm 9.68 \text{ Bqkg}^{-1}$ with an average of $193.05 \pm 7.55 \text{ Bqkg}^{-1}$ for ^{226}Ra . As for ^{232}Th , it is ranging from $8.93 \pm 0.70 \text{ Bqkg}^{-1}$ to $10.25 \pm 0.89 \text{ Bqkg}^{-1}$ with an average of $9.58 \pm 0.99 \text{ Bqkg}^{-1}$ and that of ^{40}K ranges from $99.00 \pm 5.42 \text{ Bqkg}^{-1}$ to $113.65 \pm 4.54 \text{ Bqkg}^{-1}$ with an average of $108.72 \pm 3.96 \text{ Bqkg}^{-1}$, both averages for ^{232}Th and ^{40}K are in agreement with the worldwide value documented at 30 and 400 Bqkg^{-1} respectively⁽¹⁾. It can be seen that the highest activity concentration of ^{238}U , ^{226}Ra and ^{232}Th are $237.75 \pm 24.23 \text{ Bqkg}^{-1}$, $209.78 \pm 9.68 \text{ Bqkg}^{-1}$ and $10.25 \pm 0.89 \text{ Bqkg}^{-1}$, respectively which were registered in site 2 while ^{40}K is registered in site 1 with a value of $399.96 \pm 5.38 \text{ Bqkg}^{-1}$.

The mean activity concentration for ^{232}Th was close in values as recorded in the mineralized and non-mineralized groups, which is attributed to its immobility to be altered.

The most contribution in the mineralized group (site 1) is ^{40}K with percentage of (89%), followed by ^{226}Ra (9%) and ^{232}Th (2%) as shown in fig.(2a). While fig.(2b) shows that the ^{238}U is the most contribution in the non-mineralized group (site 2) with percentage of (39%), followed by ^{226}Ra (38%), ^{40}K (21%) and ^{232}Th (2%).

The ratio $^{226}\text{Ra} / ^{238}\text{U}$ is nearly around unity in the non-mineralized hosting rocks, which means that the uranium migration-in and migration-out is nearly the same. The $^{238}\text{U}/^{232}\text{Th}$ ratio is ranged between 17.49 and 23.51 which mean that there is a migration of uranium to the hosting rocks. The disequilibrium between ^{226}Ra and ^{238}U is very clear in the mineralized samples as the ^{238}U is under limit of detection, while ^{226}Ra ranges between 28.8 Bqkg^{-1} and 43.1 Bqkg^{-1} , which means migration-out of uranium.

Mineralogy and its reflection on radionuclides distribution

XRD was made for two samples, one mineralized sample (S-1-1) from site 1 and the other is non mineralized sample (S-2-3) from site 2. The results are shown in (figs.3 and 4). The sample (S-1-1) (fig.3) which represents the mineralized group contains Hemimorphite $\{\text{Zn}_4\text{Si}_2\text{O}_7 (\text{OH})_2 (\text{H}_2\text{O})\}$ (55.7%), Hydrozincite $\{\text{Zn}_5(\text{OH})_6(\text{CO}_3)\}$ (30.2%) and Calcite, $\{\text{CaCO}_3\}$ (14.1%). These minerals are formed during the alteration processes (oxidation) for the primary hypogene minerals⁽⁴⁾. While the mineral constituents of the sample (S-2-3) which represent the non-mineralized group (fig.4) are mainly Minamlite

$\{\text{Na}_{36}\text{K}_1\text{Ca}_{27}\}$ $\{\text{Al}_3 (\text{SO}_4)_2 (\text{OH})_6\}$ (56.3%), Hematite $\{\text{Fe}_2\text{O}_3\}$ (12.9%), Kaolinite $\{\text{Al}_2\text{Si}_2\text{O}_5(\text{OH})_4\}$ (23.6%) and Anatase $\{\text{TiO}_2\}$ (7.2%).

Soliman and Hassan⁽³⁾ in their study on Gabal El Rousas reached the conclusion that high concentration of lead (Pb) meets low concentration of Zinc (Zn) and vice-versa. As it is known that the existence of radium is associated with the existence of lead and based on the above conclusion, and since in our study there is high concentration of Zinc in site1, therefore, it can be interpreted as low concentration of radium which is the case with mineralized samples understudy.

In site 2, one of the main constituent minerals is the hematite which is a ferric oxide (Fe_2O_3). Uranium is usually associated with ferric iron as adsorbed ions and so the hosting sediments have high uranium content than the mineralized, as it contains hematite (12.9%).

Hazard indices

The activity concentration values of ^{226}Ra , ^{232}Th and ^{40}K of the studied areas can be used to calculate the total gamma absorbed dose rate in air at 1 m above the ground. As shown in table (2), the average absorbed dose rate value calculated by using equation (3) for site 1 varies from 30.25 to 41.86 nGyh^{-1} with an average value of 34.85 nGyh^{-1} that is in agreement with the world wide value (59 nGyh^{-1})⁽¹⁾. Consequently, the annual effective dose range is recorded by using equation (4) to be from 0.04 to 0.05 mSvy^{-1} with an average value of 0.04 mSvy^{-1} which is also in agreement with the world wide value (0.5 mSvy^{-1})⁽¹⁾.

The average absorbed dose rate value for hosting rocks in site 2 varies from 89.21 to 107.85 nGyh^{-1} with an average value of 99.51 nGyh^{-1} using equation (3) that is in disagreement with the world wide value (59 nGyh^{-1})⁽¹⁾, accordingly, using equation (4), the annual effective dose ranges from 0.11 to 0.13 mSvy^{-1} with an average value of 0.12 mSvy^{-1} which is in agreement with the world wide value (0.5 mSvy^{-1})⁽¹⁾. For both mineralized samples (site 1) and non-mineralized samples (site 2), the average values for the annual effective dose are 0.04 and 0.12 mSvy^{-1} respectively which are less than the average recommended value (0.5 mSvy^{-1}) considering that this is in good agreement with the average world wide limits⁽¹⁾.

Radium equivalent activity (Raeq) is a widely used hazard index and it is calculated as given by equation (5). Table (2) summarized the average Raeq results for all studied samples. For the mineralized group (site 1), these values varied from 59.67 Bqkg^{-1} to 83.57 Bqkg^{-1} with an average value of 69.29 Bqkg^{-1} . As for the non-mineralized group (site 2), the average Raeq varied from 192.18 Bqkg^{-1} to 232.39

Bqkg⁻¹ with an average of 214.36 Bqkg⁻¹. The estimated average values in the present work are lower than the recommended maximum value of 370 Bqkg⁻¹ (11). By comparison with measured average values from some other countries, it is observed that the average value of this work is lower than the measured values of 366.9 Bqkg⁻¹ at southeast part of Eskisehir, Turkey (15), 266 Bqkg⁻¹ in Xiazhuang Granite Area (China) (2) and 493.8 Bqkg⁻¹ at eastern desert of Egypt (16). On the other hand the average value in the present work is higher than the measured value of 122.79 Bqkg⁻¹ in sandstone at southwestern Sinai, Egypt (17).

The radioactivity level index I_γ calculated by equation (6) in site1 is less than unity which is in agreement with the recommended value, while in site

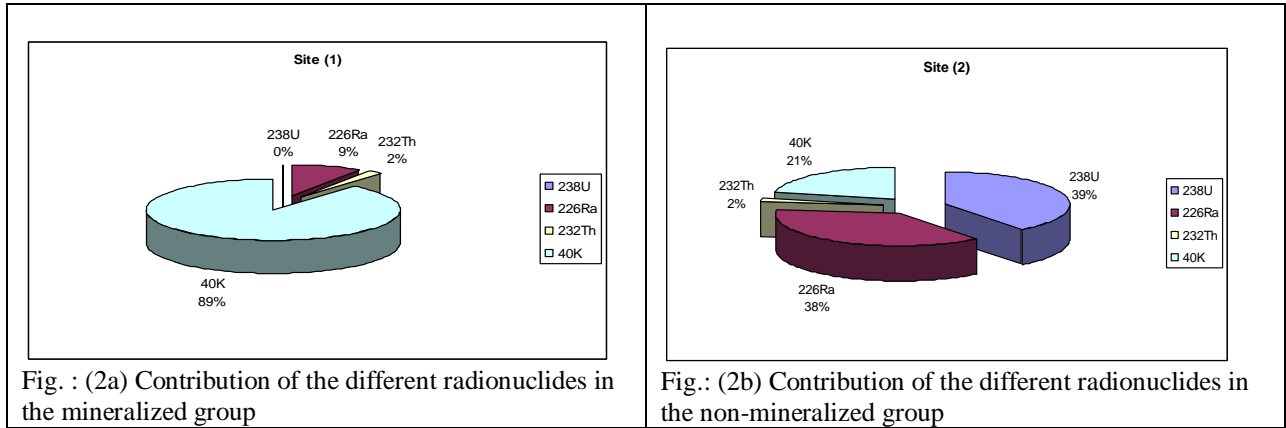
2 it is greater than the recommended value (11). There are some limited cases where the absorbed dose and the radioactivity level index I_γ do exceed the normal level of the province of Gabal El Rousas due to the presence of uranium in site 2.

The external hazard was calculated by equation (7) and it must not exceed the limit of unity for the radiation hazard to be negligible which is the case for our results for both sites as they are less than unity hence; they are in agreement with the world wide limit (10). It can be seen through Table 2 that the values of the average absorbed dose rate, annual effective dose, radium equivalent activity, radioactivity level index and that of the external hazard, in the non-mineralized group, were nearly three times those recorded in the mineralized group.

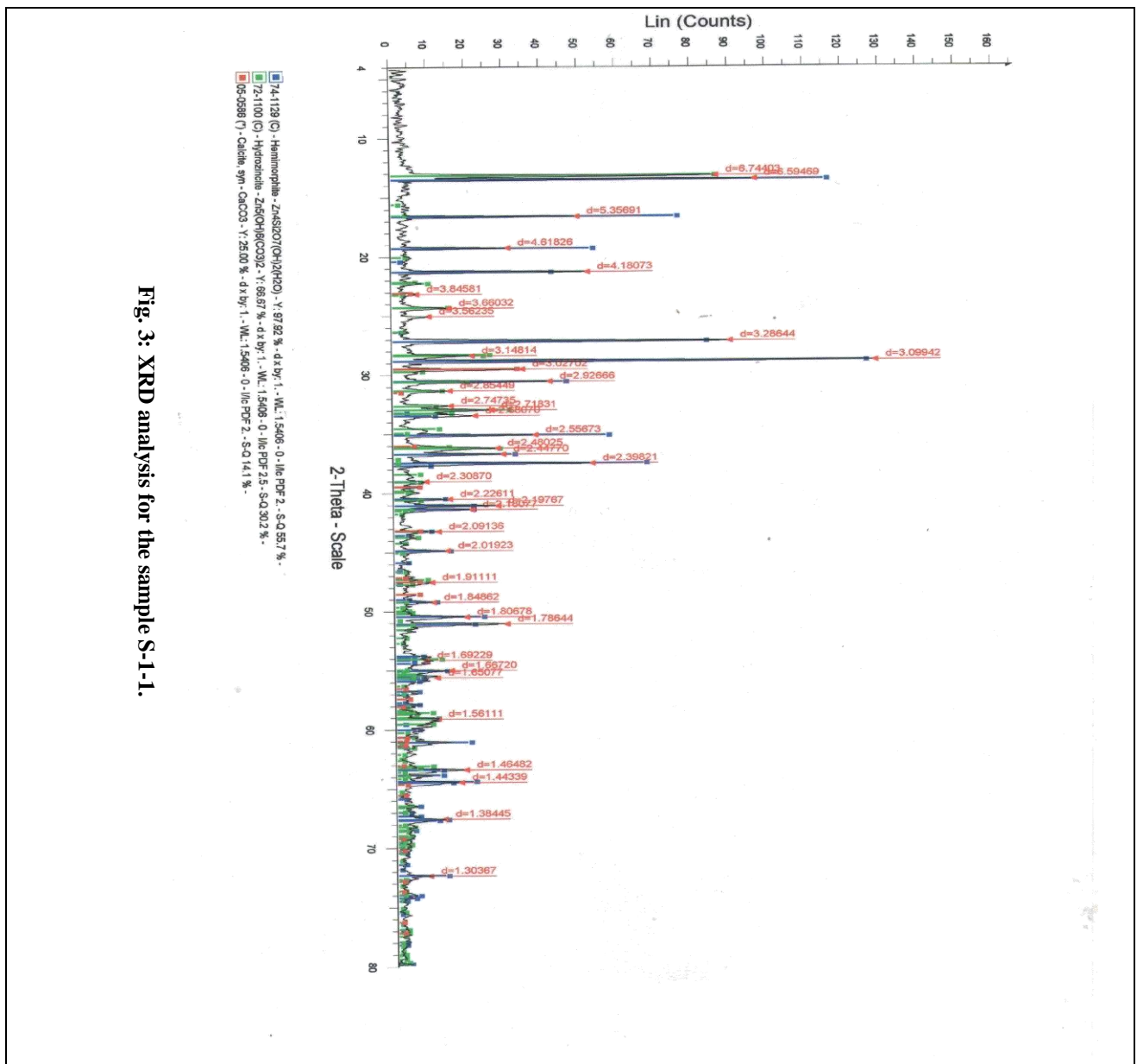
Table (1): Activity (Bq kg⁻¹) and ratios between Radionuclides for the studied samples.

Sample	234mPa		226Ra subseries Bq/Kg			232Th series Bq/Kg		Average	40K Bq/Kg	226Ra/238U 238U/232Th
	Bq/Kg	ULD*	226Ra	214Bi	214Pb	228Ac	208Tl			
S-1-1	32.06±3.26	ULD*	16.40±0.81	15.03±0.46	5.51±0.58	6.18±0.75	5.84±0.66	325.83±3.42		
S-1-2	31.22±2.76	ULD	17.37±0.79	18.67±0.28	5.52±0.60	8.04±0.37	6.78±0.48	327.10±3.35		
S-1-3	28.80±3.58	ULD	18.69±0.90	15.64±0.41	6.10±0.62	6.53±0.85	6.31±0.74	321.59±3.50		
S-1-4	41.59±8.43	ULD	20.15±1.55	19.10±0.66	6.57±1.10	9.89±1.11	8.23±1.10	399.96±5.38		
S-1-5	43.10±8.18	ULD	19.52±1.34	18.16±0.51	6.27±0.96	8.73±0.87	7.50±0.92	355.47±4.72		
S-1-6	33.07±9.19	ULD	17.96±1.54	20.67±0.61	7.24±1.54	10.22±0.99	8.73±1.26	346.31±5.17		
S-1-7	31.55±2.89	ULD	17.46±0.69	19.56±0.06	6.40±0.55	9.22±0.38	7.81±0.46	357.87±3.52		
Site (1)	34.48±5.47	ULD	18.22±1.09	18.12±0.43	6.23±0.85	8.40±0.76	7.31±0.80	347.73±4.15		
S-2-1	198.60±19.98		201.96±5.54	159.76±1.92	156.60±1.08	8.05±0.88	9.81±0.52	111.63±2.99	1.02	22.25
S-2-2	236.87±18.78		172.73±3.90	164.02±1.56	158.23±0.86	7.54±0.76	12.61±0.41	109.60±2.47	0.73	23.51
S-2-3	160.94±24.33		172.49±9.87	168.25±2.50	181.93±1.64	7.66±1.43	10.75±0.79	113.65±4.54	1.07	17.49
S-2-4	209.17±30.06		200.97±9.87	163.86±2.64	177.48±1.66	8.02±1.33	11.34±1.26	105.61±4.94	0.96	21.6
S-2-5	167.68±37.25		209.78±9.68	149.53±2.47	162.68±1.73	7.79±1.59	10.86±1.07	99.00±5.42	1.25	17.98
S-2-6	237.75±24.23		200.37±6.44	165.25±2.01	174.55±1.24	9.23±1.16	11.27±0.63	112.85±3.39	0.84	23.2
Site (2)	201.84±25.77		193.05±7.55	161.78±2.18	168.58±1.37	8.05±1.19	11.11±0.78	108.72±3.96	0.98	21.00

ULD* represents the Under Limit of Detection



Figs: (2a and 2b) Contribution of the different radionuclides for the studied area



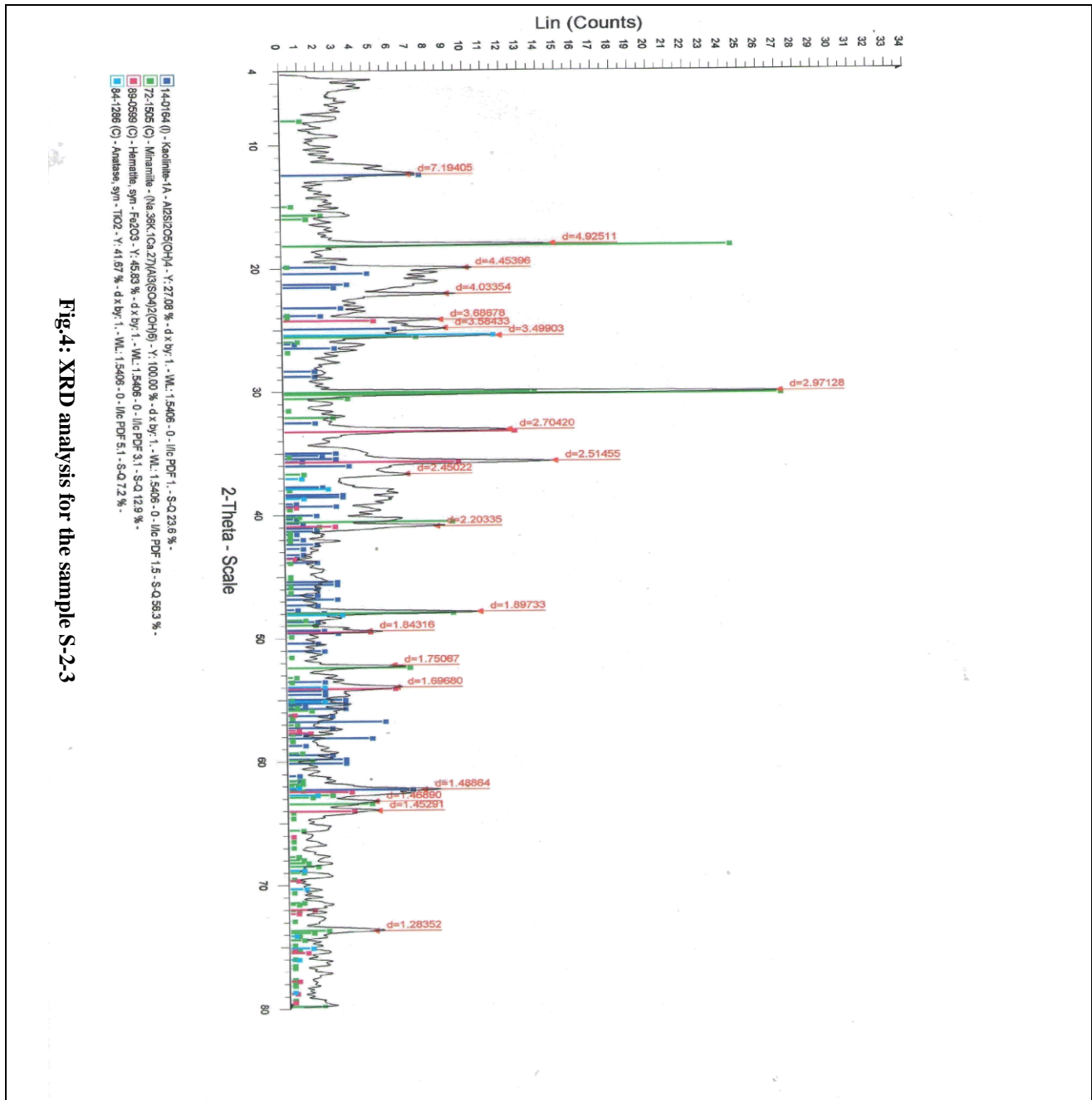


Fig.4: XRD analysis for the sample S-2-3

Table (2): The range and the average of absorbed dose rate (D), annual effective dose (E_{ff}), radium equivalent activity (Raeq), radioactivity level index (I_γ) and external radiation hazard index (H_{ex}) for the studied samples

Hazard indices	Mineralized group (N* = 7)		Non-mineralized group (N* = 6)	
	Range	Average	Range	Average
D (nGyh ⁻¹)	30.25 – 41.86	34.85	89.21 -107.85	99.51
E _{ff} (mSvy ⁻¹)	0.04 - 0.05	0.04	0.11 - 0.13	0.12
Raeq (Bqkg ⁻¹)	59.67 – 83.57	69.29	192.18 -232.39	214.36
I _γ	0.46 - 0.64	0.53	1.31 - 1.58	1.46
H _{ex}	0.17 - 0.23	0.19	0.52 - 0.63	0.58

N* represents the number of samples

Conclusion

In conclusion, this study covered the analysis of 13 samples for mineralized and non mineralized groups and reached the following:

- (1) The specific activity of ^{40}K is the largest contributor activity for the mineralized group, while both the ^{238}U and ^{226}Ra are the largest contributors for the non-mineralized group.
- (2) The average activity concentrations of ^{238}U in non-mineralized groups are higher than the world wide limit due to its association with the ferric iron mineral (hematite).
- (3) The average activity concentrations of ^{232}Th and ^{40}K for both the mineralized and the non-mineralized groups are in agreement with the world wide limits.
- (4) The estimated average for the absorbed dose rates, annual effective dose, radium equivalent activity, radioactivity level index and the external hazard index in hosting sedimentary rocks are three times higher than those in the mineralized samples.
- (5) The average absorbed dose rates and radioactivity level index of hosting sedimentary rocks are higher than the worldwide limit due to the effect of hydrothermal solution on the Miocene sedimentary rocks and its redistribution due to secondary alteration processes.
- (6) The (XRD) data for the mineralized sample (S-1-1) states the presence of major contents of Hemimorphite (55.7 %), Hydrozincite (30.2 %) and Calcite (14.1%), all played their roles in the distribution of radium.
- (7) The (XRD) data for the non-mineralized sample (S-2-3) states the presence of major contents of minamlite (56.3%) followed by Kaolinite (23.6%), Hematite (12.9%), and Anatse (7.2%), which played their role in the distribution of uranium.

Corresponding author

Sh.M.Talaat

Faculty of Women, for Art, Science and Education, Ain Shams University, Cairo, Egypt.

Shadia_talaat@yahoo.com

References

1. UNSCEAR; United Nations Scientific Committee on the Effects of Atomic Radiation, Sources and Effects of Ionizing Radiation. Report to the General Assembly with Scientific Annexes. United Nations, New York (2000).
2. Yang YX, Wu XM, Jiang ZY, Wang WX, Lu JG, Lin J, Wang LM, Hsia YF; Radioactivity concentration in soils of the Xiazhuang granite area, China. *Appl Radiat Isot.*, 63: 255 (2005).
3. Soliman M.S. and Hassan M.M.; Geology and geochemistry of the Pb and Zn mineralization in Gabal El Rousas., Ranga and Abu Anz areas, Eastern Desert, Egypt. 5th Arab science Congress, Damascus (1970).
4. Hassan M.M.; Studies on Lead-Zinc sulphide mineralization in the Red Sea coastal zone, Egypt. Proceeding, 8th IAGOD Symp., Ottawa, Canada (1990).
5. Abbady A.G.E., Uosif M.A.M., El-Taher A.; Natural radioactivity and dose assessment for phosphate rocks from Wadi EL-Mashash and El-Mahamid Mines, Egypt. *J. Environ. Radiat.* 84: 65 (2005).
6. Yucel H., Cetiner M.A., Demirel H.; Use of the 1001 keV peak of $^{234\text{m}}\text{Pa}$ daughter of ^{238}U in measurement of uranium concentration by HPGe gamma-ray spectrometry. *Nucl Instrum Method Phys Res A* 413:74 (1998).
7. Merdanoglu B., Altinsoy, N.; Radioactivity concentration and dose assessment for soil samples from Kestanbole granite area, Turkey. *Radiat. Prot. Dosimetry* 121 (4): 399 (2006).
8. Jibiri N.N., Farai P.I., Alausa K.S; Estimation of annual effective dose due to natural radioactive elements in ingestion of food stuffs in tin mining area of Jos-Plateau, Nigeria. *J. Environ. Radiat.* 94: 31 (2007).
9. Jibiri N.N., Bankole S.O.; Soil radioactivity and radiation absorbed dose rates at roadsides in high-traffic density areas in Ibadan Metropolis, southwestern Nigeria. *Radiat. Prot. Dosimetry* 118, 453 (2006).
10. Huy N.Q., Luyen T.V.; Study on external exposure doses from terrestrial radioactivity in southern Vietnam. *Radiat. Prot. Dosimetry* 118, 331(2006).
11. Organization for Economic Cooperation and Development, Exposure to radiation from the natural radioactivity in building materials. Report by a Group of Experts of the OECD Nuclear Energy Agency. OECD, Paris, France (1979).
12. Sutherland R.A., de Jong E.; Statistical analysis of gamma emitting radionuclide concentrations for three fields in Southern Saskatchewan, Canada. *Health Phys* 58, 417 (1990).
13. Papachristodoulou CA., Assimakopoulos P.A., Patronis N.E., Ioannides K.G.; Use of HPGe gamma-ray spectrometry to assess the isotopic composition of uranium in soils. *J. Environ Radioact* 64(2-3):195 (2003).
14. Zhang W., Yi J., Mekarski P., Ungar K., Hauck B., Kramer G.H.; A gamma-gamma coincidence spectrometric method for rapid characterization of uranium isotopic fingerprints. *J Radioanal Nucl Chem.* 288, Issue 1,43-47 (2011).
15. Orgun Y., Altinsoy N., Gultekin A.H., Karahan G., Celebi N.; Natural radio activity levels in granitic plutons and groundwater in Southeast part of Eskisehir, Turkey. *App. Radiat. Isot.* 63:267 (2005).
16. Arafa W., Specific activity and hazards of granite samples collected from the Eastern Desert of Egypt. *J. Environ Radioact.* 75:315-327 (2004)
17. ElAassy I.E., ElGaly M.M., Nada A.A., El Feky M.G., Abd El Maksoud T.M., Talaat Sh. M and Ibrahim E.M.; Effect of alteration processes on the distribution of radionuclides in uraniumiferous sedimentary rocks and their environmental impact, southwestern Sinai, Egypt. *J Radioanal Nucl Chem;* 289 n.1, 173- 184 (2011).